ELSEVIER

Medical Engineering & Physics 24 (2002) 337–347

Medical Engineering & Physics

www.elsevier.com/locate/medengphy

Optimizing the biomechanical compatibility of orthopedic screws for bone fracture fixation

A. Gefen *

Department of Biomedical Engineering, Faculty of Engineering, Tel Aviv University, Tel Aviv 69978, Israel

Received 17 August 2001; received in revised form 31 January 2002; accepted 7 March 2002

Abstract

Progressive loosening of bone fixation screws is a well-documented phenomenon, induced by stress shielding and subsequent adaptive bone remodeling which results in bone loss around the screw. A set of two-dimensional computational (finite element) models was developed in order to test the effect of various engineering designs of fixation screws on the predicted screw–bone stress transfer, and consequently, on the biomechanical conditions for osteosynthesis. A dimensionless set of stress-transfer parameters (STP) was developed to quantify the screw–bone load sharing, enabling a convenient rating to be given of the biomechanical compatibility of practically any given screw design according to the nature of the simulated mechanical interaction. The results indicated that newly proposed screw designs, i.e. a 'graded-stiffness' composite screw with a reduced-stiffness-titanium core and outer polymeric threads and an 'active-compression' hollow screw which generates compressive stresses on the surrounding bone, are expected to provide significantly better biomechanical performances in terms of the STP criteria, compared with conservative screw designs. Accordingly, the present work demonstrates that finite element computer simulations can be used as a powerful tool for design and evaluation of bone screws, including geometrical features, material characteristics and even coatings.

Keywords: Stress shielding; Osseointegration; Osteosynthesis; Bone modeling/remodeling; Finite element analysis

1. Introduction

Bone screws are clinically accepted and widely used devices for fixation of bone fractures or for stabilizing bone transplants. In this simple type of fixation, the screw glides into one bone fragment, which is thus united with another fragment by compressing against it when the screw is tightened (Fig. 1(a)). However, since the screw remains attached to the bony tissue after it was healed, it may also diminish the bone's strength and stiffness. The significantly stiffer metallic screw (elastic modulus of 100–200 GPa) carries most of the shared load, causing the adjacent bone (elastic modulus of 1–20 GPa) to be atrophied in response to the diminished load it is carrying, in accordance with Wolff's law of functional adaptation (Fig. 1(b)). This effect of metallic screws on the bony tissue in their vicinity is called 'stress shielding'. The 'biomechanical compatibility' of a particular screw with bone can, therefore, be characterized by the stress distribution developing in the bone around the screw as a result of the screw's tightening during implantation.

Many in vitro studies concerned the holding power of screws, quantified by means of pullout tests. The pullout resistance of screws was shown to be strongly dependent on the thread design. Since the volume of bone bounded between the threads of the screw determines the resistance to the shearing loads during pullout, the profile shape, depth of threads, number of threads and distance between threads may all critically affect the pullout resistance. For a similar reason, longer screws will increase the pullout resistance and strength [1–6]. Pullout tests, however, provide only limited information about the screw–bone contact conditions, and cannot be utilized to locate stress concentrations in the screw or bone, or be applied for optimizing the screw–bone load sharing. Apparently, computational simulations are the most feasible approach for analysis of these factors.

* Tel.: +972-3-640-8093; fax: +972-3-640-5845.
E-mail address: gefen@eng.tau.ac.il (A. Gefen).

1350-4533/02/$22.00
PII: S1350-4533(02)00027-9

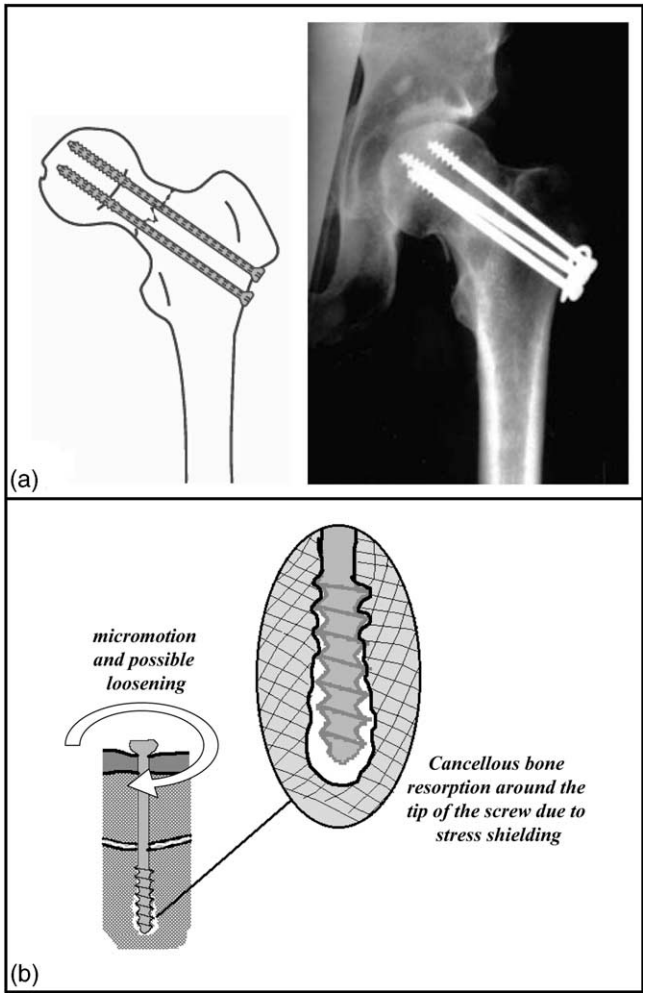

Fig. 1. Bone fracture fixation: (a) schematic description (left) and post-surgical X-ray imaging (right) of screw fixation of a femoral neck fracture; (b) an illustration of the process leading to failure of the fixation as a result of lack of biomechanical compatibility between the screw and surrounding cancellous bone.

A number of experiments with screw and plate fixation systems have shown that cortical and trabecular bone losses in canine models are reduced if a reduced-stiffness-implant with identical geometrical design is being used [7,8]. Cushioning the fixation with a silicone layer to reduce its overall stiffness was further shown to minimize underlying bone resorption [9]. Van Reitbergen et al. [10] demonstrated that metallic (titanium) hip stems implanted in dogs caused 20–23% reduction in proximal femoral bone cross-section two years post-implantation. Recently, Ang et al. [11] compared bone remodeling around metallic and polymeric hip stems in humans using DEXA and showed greater bone mineral density around the polymeric (less stiff) stems, which allowed bone to share increased loading. These animal and patient studies strongly support the hypothesis that lack of mechanical stimuli to bone due to stress shielding will cause its progressive absorption around the implant. Thus, optimization of the design of screws to induce stress in the bone layers enveloping the implant, and in particular, within the bone volumes that are bounded between the threads of screws may minimize the risk for loosening.

In 1985, more than 20% of the orthopedic beds in European countries were taken by cases of proximal femur fractures, 50% of which treated by internal screw fixation (Fig. 1(a)). Since 1985, these numbers have risen and will be significantly higher in the coming decades, with the aging of the population [12]. A recent statement from the American Academy of Orthopaedic Surgeons [13] suggests that the current annual US figure of 350,000 hip fractures is likely to rise to 650,000 by 2050. The success of fixation procedures depends mainly on the holding power of the screws. Presently, there is a concern among surgeons about the risks involved when fixation fails due to loosening of the screws caused by stress shielding. In screw fixation following trauma of the spine, for example, loosening may endanger tracheoesophageal structures and could even require immediate removal of the failing implant [14]. This may impose a prolonged and painful rehabilitation process for patients, as well as high-costs for health services. In order to overcome these problems, new concepts for fixative screw design that consider minimization of stress shielding effects are required.

Although a significant number of cases of screw loosening have been reported [14–17], conservative bone screw designs that were available in the market for internal fixation during the past three decades generally provided favorable mechanical results [18,19]. However, according to the author's knowledge, the effects of the screw's various engineering designs (including both geometrical and material characteristics) on the mechanical screw–bone interaction have not been studied comprehensively. Moreover, no standard method is available for comparing the biomechanical compatibilities of the different commercially available designs. Analyses of the stress distributions in bony tissue around fixation screws have so far been limited to optical and computational evaluations of the contact conditions in the region under the head of an 'anchor-type' screw [20] or to evaluation of preferable screw diameters for osteotomy of the mandible [21–23].

Therefore, the first goal of this study was to characterize general screw designs that could minimize stress shielding by allowing similar loads to be shared between the screw and the surrounding bone, and by providing a more uniform stress state within the bone, which is expected to generate the mechanical stimuli for adequate bone modeling and osseointegration. A second goal of this study was to develop a dimensionless parametric evaluation method for comparing and rating the biomechanical compatibilities of various screw designs, which may differ by their geometrical and/or material properties. In order to achieve these goals, the stress states pro-

duced by the mechanical interactions of bone with different structural designs of screws were evaluated by means of two-dimensional (2D) computational models solved using the finite element (FE) method. In these models, the von Mises comparative stresses were calculated, so as to predict the screw–bone load sharing, and consequently, the conditions for bone modeling/remodeling. The present approach of optimizing the stress transfer to the bone in the vicinity of the screw is expected to alleviate the above-described conditions of loosening and failure of fixations due to stress shielding.

2. Methods

2.1. Rationale

Two FE model types of the screw–bone interaction were developed. The first is an idealized 2D axisymmetrical model of a bone cylinder with an outer cortical surface and an inner trabecular bulk (Fig. 2(a)). A screw is inserted perpendicularly to the bone surface, loading the modeled bone with axial tensile force and screw-to-bone contact conditions. This not only permitted easy creation of models, but also provided a tool for basic comparisons of screw performances, by isolating the effects of the screw's engineering design parameters. Other structural and physiological effects (e.g. those of the complex musculoskeletal loading system) could thereby be excluded. The second model type was selected to be that of the proximal femur, implanted with different screw types (Fig. 2(b)). The latter modeling approach was selected because the musculoskeletal loading system of the hip joint had been comprehensively studied by others and may be regarded as a benchmark problem in the field of metallic orthopedic implants, thus allowing extensive comparisons with previously published computational and clinical results.

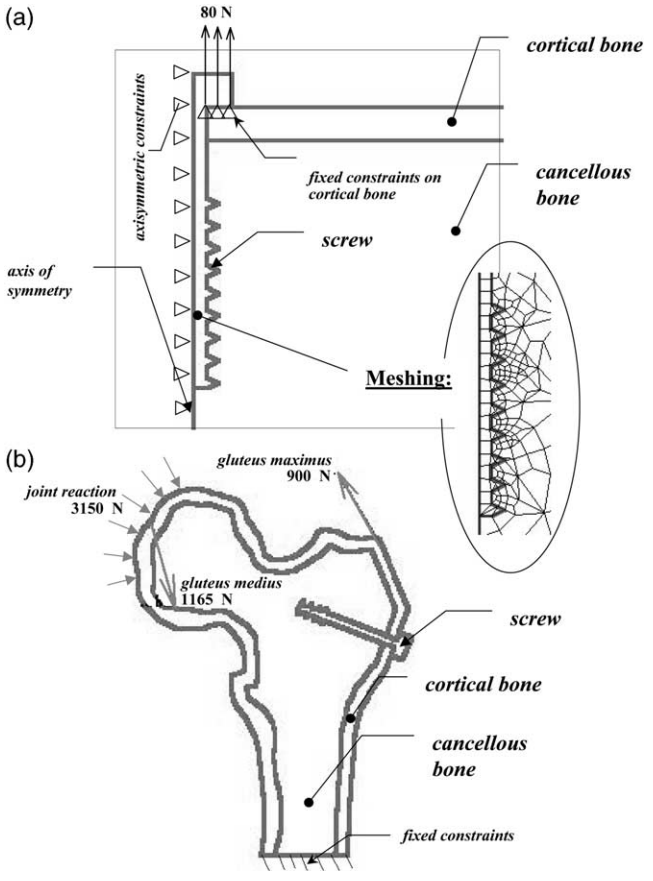

Fig. 2. Two-dimensional computational modeling of the screw–bone mechanical interaction: (a) idealized model and (b) femoral head model.

2.2. Design of bone screws

The basic dimensions of the screws were selected to represent commercially available designs. The following dimensions were set constant throughout the simulations: shaft diameter 2.0 mm, screw-head diameter 6.0 mm, thread pitch 1.0 mm, and screw length (including the threads, but excluding the head) 25.0 mm. Other geometrical characteristics as well as the material properties of the screw were altered in attempt to enhance the biomechanical compatibility, as follows. The profile shape of the threads was modeled as triangular, rectangular or trapezoidal, the thread diameter was taken as 4 or 6 mm, the number of threads was determined as 5 or 8, 9, and the shaft length, defined as the distance between the first (most upper) thread to the compact bone layer, was taken as 1 or 5 mm. The screws were assumed to be made of regular titanium alloy (Ti–6Al–4V) with elastic modulus of 105 GPa and Poisson ratio of 0.35, or to be made of metallurgically treated titanium with a reduced-stiffness, i.e. an elastic modulus of 40 GPa. The effect of each of the above parameters on the biomechanical compatibility of the screws was evaluated individually, using a parametric representation of the screw-to-bone stress-transfer performances, as further detailed.

The performances of two newly proposed designs were also tested (Fig. 3). The first is a 'graded-stiffness' screw (Fig. 3(b)) integrating two different components: a low-stiffness-titanium core with an elastic modulus of 40 GPa and polymeric external layer/threads with an elastic modulus of 10 or 5 GPa. The second design is an 'active-compression' hollow screw (Fig. 3(c)), in which a rigid metal sphere is contained. Following insertion of the screw, the sphere is pushed downward within its canal, thereby causing slight opening of the screw's tip that leads to transfer of compression stress to the adjacent bone. For modeling purposes, a horizontal force of 5 N was introduced at the distal third of the active-compression screw, to represent the action of this sphere. The 5 N force value was calculated by modeling the

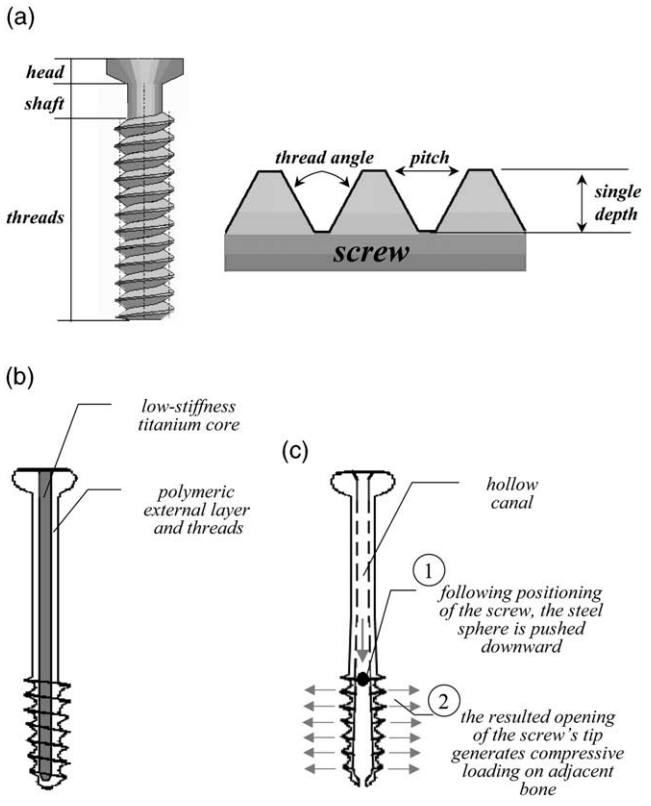

Fig. 3. Design of standard and novel screws: (a) the three main components of the standard screw include the head, shaft and the core, covered with threads. The geometrical characterization of the threads (right) includes the pitch (distance between the threads), the single depth of a thread (calculated from the root to crest of the thread), and the thread angle. The proposed cancellous screw designs include: (b) graded-stiffness screw providing gradual transfer of contact stresses to bone by means of a stiff metallic core and a softer polymeric external layer and (c) active-compression screw providing mechanical stress stimuli for growth and osteosynthesis of adjacent bone.

canal wall of the active-compression screw as a cantilever beam subjected to bending due to thrusting of the sphere; the maximal bending compression generated within the canal wall of the active-compression screw was limited to 50% the compressive strength of trabecular bone (~10 MPa), for eliminating potential local tissue damage while activating this screw.

The aforementioned two new designs, graded-stiffness and active-compression, are likely to improve the stress transfer to the bony tissue in their vicinity. The former design may minimize stress shielding by enabling a more gradual stress reduction from the metallic core to the bone, while the latter design could enhance osteosynthesis around the screw by providing a mechanical compression stimulus for local bone modeling and growth around the screw.

2.3. Finite element analyses

Axisymmetric idealized models were initially developed to isolate the effects of the screw's engineering design on the stress transfer to bone. Subsequently, performances of the different screws were tested in a more realistic geometry of the proximal femur. The following basic components were included in each idealized axisymmetric simulation (Fig. 2(a)): (i) uniform 3 mm layer of compact bone, (ii) underlying homogenous bulk representing trabecular bone and (iii) fixation screw. The selected thickness of the compact bone layer is typical for the femur and tibia [20]. The bony tissue was assumed to be linear elastic, with moduli of 20 GPa for the cortical layer and 1 GPa for the trabecular bulk, and with a Poisson ratio of 0.35 [24]. The axisymmetric idealized models were constrained for horizontal displacement (but not for vertical sagging) along the axis of symmetry of the screw (Fig. 2(a)). Surfaces of the opposite boundary and the base of these models were constrained for both vertical and horizontal displacements. The upper surface, to which screws were inserted, was left free to deform under the contact loading transferred through tightening of the screw. The transfer of tightening load to bone was simulated by fixing the lower part of the screw's head to the cortical surface so that each node of the FE mesh at the contacting surface of the screw's head was matched with a node at the cortical surface directly underneath it. The translation and rotation displacements of each pair of such nodes were imposed to be equal. On each simulation, the surface under the screw's head was loaded with a force of 80 N distributed over the pairs of nodes in the screw and bone meshes, in order to simulate tightening [20].

The more complex 2D model of a fixative screw inserted into the femoral head was reconstructed from an anatomical scheme (Fig. 2(b)). This model type was aimed to include additional structural factors that may affect the screw–bone stress transfer, such as the non-uniform thickness of the cortical layer and skeletal/muscular loading. The boundary conditions at the more complex models of the femoral head included similar contact analysis at the screw's head–bone interface. The femur model was fully constrained at its base, but all other surfaces were free to deform under the musculoskeletal loading and the screw's tightening load. A set of loads of 3150 N distributed over the joint surface, 900 N at 15° medially to the vertical axis and 1165 N at 30° laterally to the vertical axis was applied to the femoral head, in order to simulate the loading conditions caused by the joint reaction and the contraction of the gluteus maximus and the gluteus medius muscles, respectively, during averaged daily activities [24].

2.4. Evaluation and rating of biomechanical compatibilities of the bone screw designs

The FE models were built using the NASTRAN software package. Meshes of 250–300 or 800–1000 plate elements (2D, 4 nodes) were produced for the idealized

models and the femoral head models, respectively. At the screw–bone interface zones, finer meshing was produced to improve the accuracy of the numerical solution (Fig. 2(a)). Stress distributions were represented by the von Mises equivalent stress, σ_{vm}, which weighs the effects of both tension (σ_t) and compression (σ_c) stresses by

$$\sigma_{vm} = (\sigma_t^2 + \sigma_c^2 - \sigma_t\sigma_c)^{1/2} \quad (1)$$

In order to characterize the load transfer between the screw and the cancellous bone, towards understanding the conditions for local bone modeling/remodeling and osteosynthesis post-implantation, quantitative parameters should be defined. These parameters, which are termed as the stress-transfer parameters (STP), provide a dimensionless evaluation of the load sharing between a given fixation screw and the bone surrounding it. Two different STP, α and β, are defined (Fig. 4(a)):

$$\alpha = \frac{\sigma_{fb}}{\sigma_{ft}} \quad (2)$$

$$\beta = \left(\frac{1}{N}\sum_{i=2}^{N}\sigma_{b_i} / \frac{1}{N}\sum_{j=2}^{N}\sigma_{t_j}\right) = \left(\sum_{i=2}^{N}\sigma_{b_i} / \sum_{j=2}^{N}\sigma_{t_j}\right) \quad (3)$$

The stress transfer from the first (most upper) thread of the screw, which bears an average stress of σ_{ft}, to the cancellous bone volume that is located directly above it, and withstand an average stress of σ_{fb}, is quantified by the α STP. The stress transfer from all the other threads of the screw (indexed as $j \geq 2$ to exclude the first thread) which bear respective stresses of σ_{t_j}, to the bone volumes (indexed i) that are found between these threads and are withstanding respective stresses of σ_{b_i}, is quantified by the β STP. Since the bone is compressed between the first thread of the fixation screw and the head of the screw (Fig. 4(b)), the first thread carries a substantial load, which may cause stress concentrations to appear above it. For this reason, STP evaluations of the screw–bone stress transfer were carried out separately for the first thread (Eq. (2)), and for all other threads (Eq. (3)).

These dimensionless STP provide a convenient tool for evaluation of the stress transfer from any screw design to the surrounding bone. Ideally, for a screw made of a material with properties identical to those of the bone, the screw and the bone will share similar loads and a nearly homogeneous stress transfer will result. In this case, stress shielding will be eliminated and the values of the above-defined STP (Eqs. (2) and (3)) will approach an optimal magnitude of unity. Indeed, the idealized simulations provided values of 0.96–0.99 for both STP while modeling different hypothetical screws with triangular, rectangular or trapezoidal profiles as being fabricated from a material with an elastic modulus identical to that of cancellous bone (1 GPa). Contrarily, for screws with lower biomechanical compatibility (e.g. those that are significantly stiffer than bone), lower STP values are obtained. By this means, the dimensionless STP were utilized to rate the above-described different commercial/new screw designs and identify the design parameters that are most critical for better biomechanical performances.

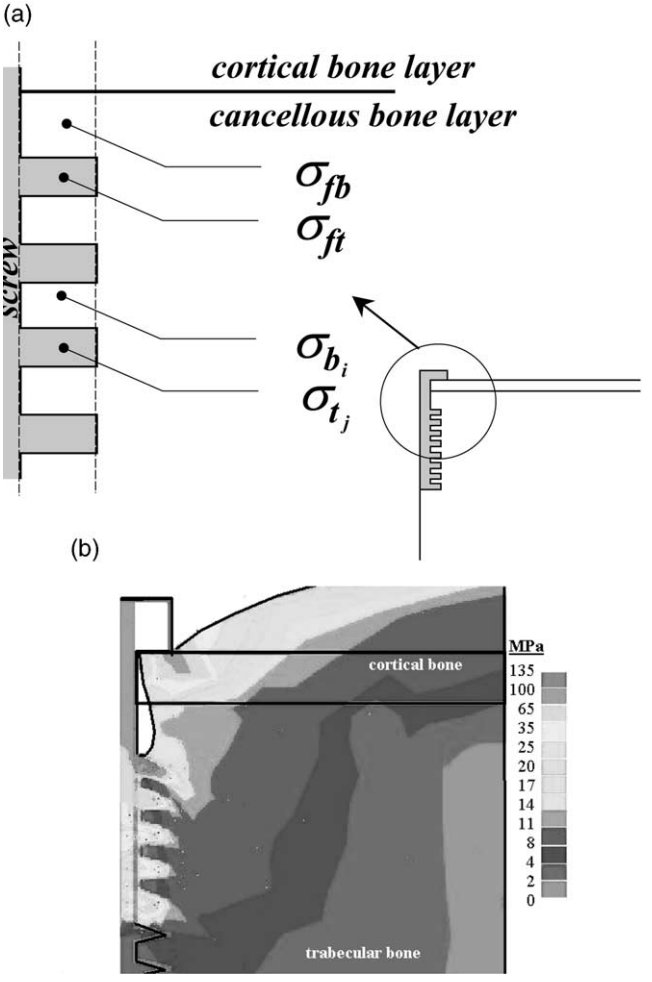

Fig. 4. Computation of the STP: (a) definition of regions for calculating the average screw–thread stress values and the average stress values within cancellous bone that is found between threads, as required for computation of the STP; (b) the bone is compressed between the screw's first thread and its head, as demonstrated in this screw–bone v.Mises stress distribution that shows the resulted bone deformation (magnified 30×, and superimposed on the boundaries of the undeformed shape). The first thread is thereby subjected to stress concentrations. For this reason, STP evaluations of the screw–bone stress transfer were carried out separately for the first thread (Eq. (2)), and for all other threads (Eq. (3)).

3. Results

The idealized and femoral head models were solved for analysis of the mechanical interaction between the bone and the different fixation screws, and the stress transfer was quantified and rated using the dimensionless

STP approach (Table 1). As detailed in Section 2, greater STP values (that are as close as possible to 1) are desired, as these will indicate a more optimal sharing of loads between the fixation screw and the surrounding cancellous bone. The effects of different design features on the biomechanical compatibility of the screws, in terms of the STP, are detailed as follows.

- *Young's modulus*. Reduction of the elastic modulus of the screws from 105 to 40 GPa resulted an averaged increase of 35% in the STP values obtained for the different screw profiles, i.e. triangular, rectangular and trapezoidal (for example, see Fig. 5). Low-stiffness screws, therefore, provided significantly improved biomechanical compatibility. Reducing the screw's elastic modulus was shown to have a generally lower influence on the STP of screws with a smaller diameter (averaged resulted increase of 13% in STP values) compared with those having a larger diameter (increase of 43% in STP values). This indicates that the critical magnitude that should be reduced in the process of engineering design, in order to improve the biomechanical compatibility of bone screws, is the structural stiffness under compression loading, which is defined as the product of the elastic modulus multiplied by the cross-sectional area (and not the elastic modulus solely).
- *Thread diameter.* The change in stress transfer as a result of increasing the diameter of the screws was shown to be dependent upon other design parameters, and mainly, upon the profile shape. For example, increasing the diameter of a screw with a triangular thread profile slightly improved the stress transfer from the first thread to the bony tissue above it (α STP increased by 6%) and significantly enhanced the stress transfer between the other threads and adjacent bone (β STP increased by 188%). Contrarily, increasing the diameter of a trapezoidal screw reduced both α and β STP values by 11 and 30%, respectively. It appears the screw diameter should be optimized, using the STP parameters, following selection of the profile shape and material properties of the screw.
- *Thread profile.* With respect to the interaction with cancellous bone, the trapezoidal profile gave the highest STP values (Fig. 6), and, thereby, demonstrated the best biomechanical compatibility (α, β STP values for the triangular profile were on average higher by 39 and 6% than the ones calculated for triangular and rectangular profile shapes, respectively). Investigation of the stress distribution on the cortical surface around screws with different profiles showed that the number of threads significantly affects the surface stresses. For all the 9-thread screws (with both short shaft and long shaft), the trapezoidal profile provided a more homogenous surface stress distribution (Fig. 6(b)), with a peak stress value that was lower by 28 and

Table 1
Performance rating (from best to worst) of different bone screws in terms of the STP α, indicating the load sharing between the first thread of the screw and the bone volume above it, and β, indicating the load sharing between all other threads and the bone bounded between them. The load sharing is considered to be optimal when the screw and the surrounding bone are carrying similar loads. In this case, the values of the STP α and β approach the unity value

Engineering design				α	β
Profile shape	No. of threads	Diameter (mm)	Elastic modulus (E) (GPa)		
Triangular	9	4	40 Active-compression	0.877	0.870
Rectangular	9	4	40 Active-compression	0.973	0.743
Trapezoidal	8	6	40(core)/5 (threads) Graded-stiffness	0.676	0.552
Trapezoidal	5	6	40(core)/5 (threads) Graded-stiffness	0.543	0.379
Trapezoidal	8	6	40(core)/10 (threads) Graded-stiffness	0.518	0.352
Trapezoidal	9	6	40 Short shaft	0.568	0.195
Trapezoidal	5	6	40(core)/10 (threads) Graded-stiffness	0.355	0.261
Rectangular	9	4	40 Short shaft	0.418	0.143
Rectangular	9	6	40 Short shaft	0.433	0.093
Rectangular	9	4	105 Short shaft	0.397	0.126
Trapezoidal	9	6	105 Short shaft	0.407	0.112
Trapezoidal	9	6	40	0.333	0.146
Triangular	9	6	40 Short shaft	0.292	0.115
Triangular	9	4	40 Short shaft	0.272	0.124
Trapezoidal	9	6	105	0.257	0.123
Rectangular	9	6	105 Short shaft	0.283	0.077
Rectangular	9	4	40	0.241	0.101
Trapezoidal	5	6	40	0.233	0.100
Rectangular	9	4	40	0.234	0.096
Rectangular	9	6	40	0.241	0.085
Triangular	9	4	105 Short shaft	0.231	0.082
Rectangular	5	6	40	0.230	0.080
Triangular	9	4	40	0.194	0.095
Rectangular	5	6	105	0.215	0.063
Rectangular	5	4	40	0.168	0.108
Rectangular	5	4	105	0.166	0.106
Triangular	9	4	105	0.183	0.079
Triangular	9	6	40	0.168	0.093
Rectangular	9	6	105	0.191	0.065
Triangular	9	6	105 Short shaft	0.170	0.068
Trapezoidal	5	6	105	0.147	0.074
Triangular	9	6	105	0.127	0.069
Triangular	5	4	40	0.121	0.074
Triangular	5	6	40	0.122	0.072
Triangular	5	4	105	0.120	0.067
Triangular	5	6	105	0.084	0.048

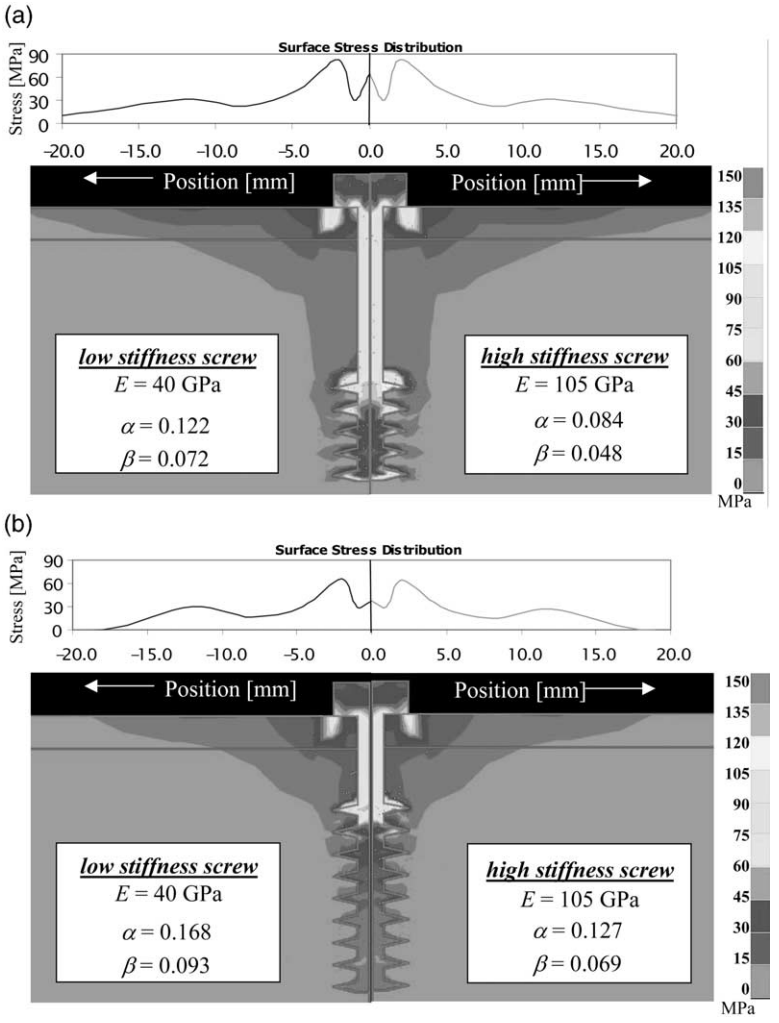

Fig. 5. Distribution of v.Mises stresses resulted by the screw–bone interaction for 6 mm screws with a triangular profile of (a) 5, and (b) 9 threads. For each of these cases, three diagrams are shown: the top is the distribution of v.Mises stresses on the cortical surfaces, the left one is the internal stress state for the more elastic screw (40 GPa) and the right one is the internal stress state for the stiffer (105 GPa) screw. Note the decrease in stress concentrations on the first screw's thread and the more homogenous loading of bone under the first thread as a result of reduction of the screw's elastic modulus from 105 to 40 GPa.

11% compared to the triangular and rectangular profiles, respectively. When the number of threads was decreased to 5, the rectangular profile was shown to generate the most homogenous surface stress distribution, with a maximal stress value that was lower by 17 and 27% compared to the ones generated by the trapezoidal and triangular profile shapes, respectively.

- *Number of threads.* In general, increasing the number of threads yielded a more continuous stress transfer between the screw and bone, demonstrated by a rise in the STP values (Figs. 5 and 6). Accordingly, the STP values of the 9-thread models were higher by 21% in average, compared to those of the 5-thread models. The stress distribution on top of the cortical layer was also improved in the 9-thread screws (Figs. 5(b) and 6(b)), providing a lower peak stress for each of the three different profile shapes tested (for example 33% reduction in the maximal stress value for the trapezoidal profile).
- *Shaft length*. The short shaft models provided better stress transfer to the cancellous bone in comparison to those with a long shaft, in terms of the STP (32% higher values in average). The stress distribution on the cortical surface was also more homogenous, demonstrating lower maximal stress values for all the different profiles tested (for example, 17% reduction in the peak stress for the trapezoidal profile as a result of shortening the shaft). However, local internal stresses within the first thread of the screw were shown to be greater by 25%, in average, in the short shaft models.
- *Graded-stiffness screw*. Design of a stiff core and more elastic outer layer/threads significantly improved the biomechanical compatibility, as quantified by the STP (Fig. 7). As the elastic modulus of

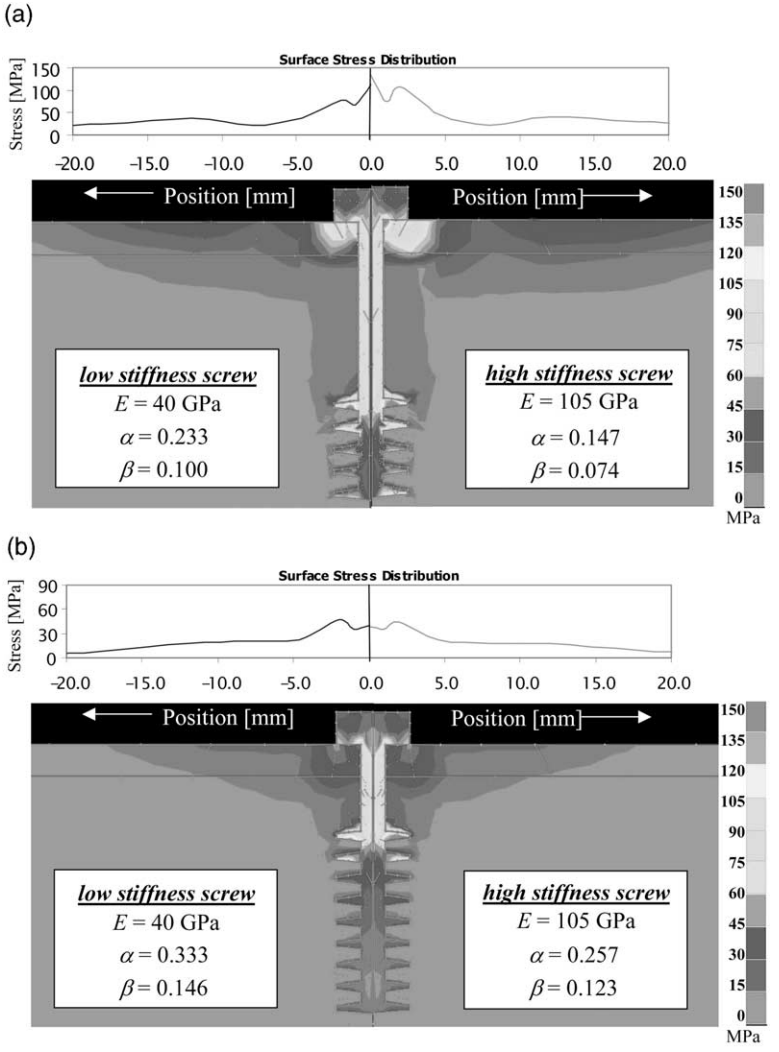

Fig. 6. Distribution of v.Mises stresses resulted by the screw–bone interaction for 6 mm screws with a trapezoidal profile of (a) 5, and (b) 9 threads. For each of these cases, three diagrams are shown: the top is the distribution of v.Mises stresses on the cortical surfaces, the left one is the internal stress state for the more elastic screw (40 GPa) and the right one is the internal stress state for the stiffer (105 GPa) screw. Note the more homogenous surface stress distribution resulted by the increase in the number of threads, from 5 to 9.

the outer component of the screw decreased (from 10 to 5 GPa), the STP values significantly increased, approaching the optimal unity value. Contrarily, decreasing the thread stiffness was shown to have almost no effect on the stress distribution developing on the cortical surface. The best performances were shown to be the ones of the 6 mm graded-stiffness screw, with 8 threads of trapezoidal profile shape, an inner reduced-stiffness-titanium core (with an elastic modulus of 40 GPa) and a soft outer polymeric coating (with an elastic modulus of 5 GPa). For this screw, the α and β STP values were considerably enhanced, being 0.676 and 0.552, respectively (Fig. 7(b), left diagram). The STP of the graded-stiffness screws were approximately 68% higher than those of single-material screws with identical overall geometry, indicating the potential in improvement of the stress transfer by using such simple composite fixations.

- *Active-compression screw*. This proposed design for a bone screw also appears to be promising, providing the best results in terms of the STP. The result of applying compressive forces to bone near the tip of the screw is, as expected, a significant improvement in the transfer of stresses from the lower threads of the screw to the surrounding tissue, which is reflected by high values of the β STP that approach the ideal unity value. For example, an idealized simulation of a 4 mm active-compression screw with a triangular profile yielded values of 0.877 and 0.870 for the α and β STP, respectively. A similar analysis of an active-compression screw with a rectangular profile yields values of 0.973 and 0.743 for the α and β STP, respectively.

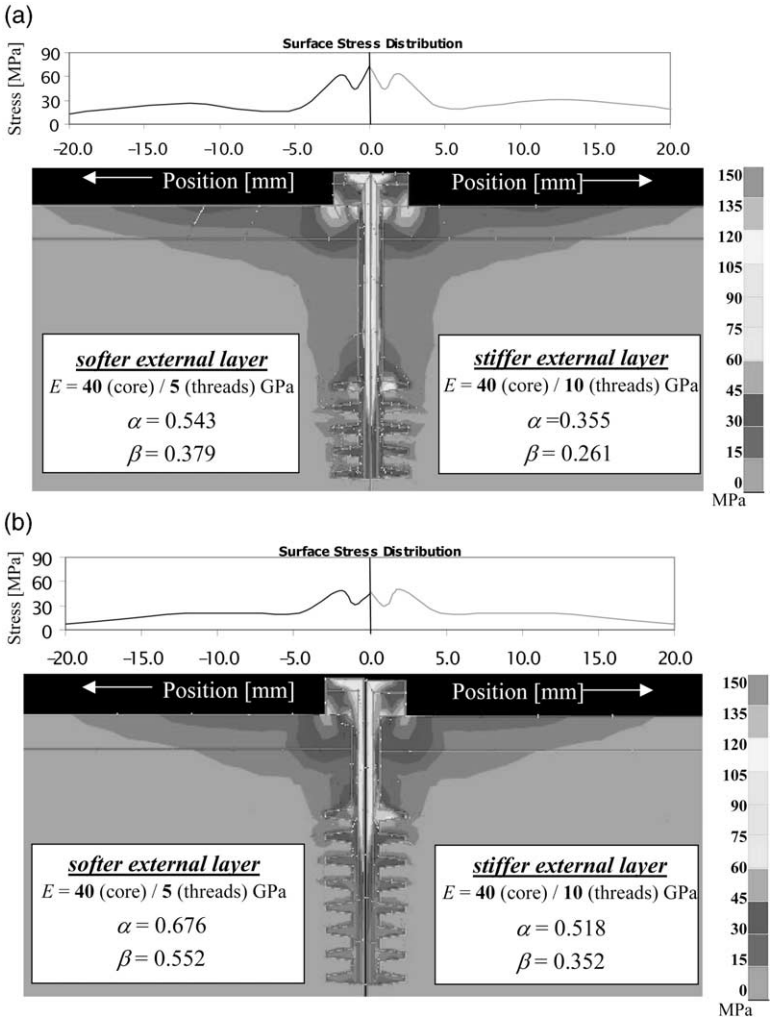

Fig. 7. Distribution of v.Mises stresses resulted by the screw–bone interaction for 6 mm graded-stiffness screws with a trapezoidal profile of (a) 5, and (b) 8 threads. For each of these cases, three diagrams are shown: the top is the distribution of v.Mises stresses on the cortical surfaces, the left one is the internal stress state for a screw with a more elastic polymeric external layer (5 GPa) and the right one is the internal stress state for a screw with a stiffer (10 GPa) external layer. Note that the STP of the graded-stiffness screws were approximately 68% higher than those of single-material screws with identical overall geometry.

- *The idealized models versus the femoral head models*. In general, comparative evaluations of different screw designs were found to be independent of the modeling approach. The relative rating of screws was maintained while using either idealized or femoral head models. However, the absolute STP values obtained for the femoral head models were significantly larger than those obtained for the idealized models. For example, using the idealized modeling approach, a 4 mm titanium screw with a rectangular profile obtained a score of 0.166 and 0.106 for the STP α and β, respectively, while using the femoral head model, it obtained larger scores, of 0.476 and 0.643 for the STP α and β, respectively. This indicates that the realistic load sharing between the screw and the surrounding bone is actually better than predicted using our idealized model. The complex system of loads that act on a screw within the proximal femur is not limited to axial forces along the screw's shaft, but also involves bending and shear, which apply additional stress on the bone bounded between the screw's threads (Fig. 8), and, consequently, provide further stimulus for bone modeling and osseointegration. In view of these factors, it was concluded that maintaining consistency in the modeling approach is a basic condition for utilizing the STP comparative evaluations.

4. Discussion

A method of evaluating and rating engineering designs and expected biomechanical performances of orthopedic fixative screws was presented. The results indicated that two newly proposed designs, a graded-stiffness composite screw and an active-compression screw are expected to be of superior biomechanical com-

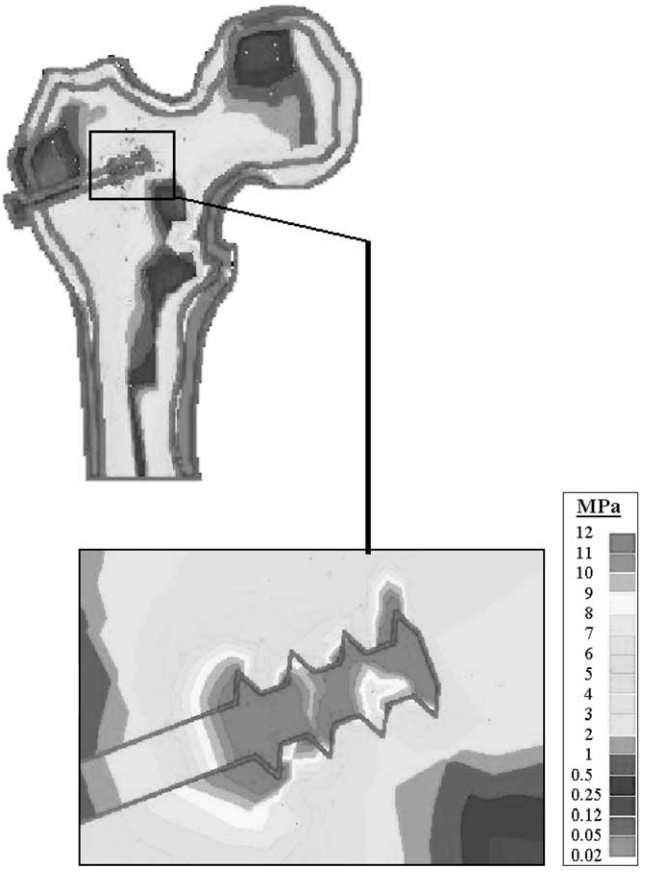

Fig. 8. The v.Mises stress distribution within the 2D computational model of the femoral head following implantation of a fixation screw (top), and the magnified stress transfer to bony tissue around the triangular 4-thread profile of the screw (bottom).

patibility with bone in respect to conservative bone screw types with triangular, rectangular or trapezoidal profile shapes. The rating of STP performances of the many screw designs tested was consistent while testing it in two simulation types, i.e. idealized and femoral head models. The author believes that these similar trends suggest that the STP approach of quantifying the screw-bone stress transfer may have a certain universal validity.

The results had shown that for all the screw designs tested, the peak stress region occurred within or right before the first thread. This is consistent with most clinical failures, where the screw was broken [25]. In general, these maximum regional stresses increased as the length of the screw's shaft decreased. Experimental pull-out tests carried out to evaluate the holding power of commercially available screw designs revealed that increasing the number and density of threads significantly improves the holding power of the screw within cancellous bone [26]. Increasing the number of threads and the length of the screw also reduced the stress concentrations within the first thread [25]. The present findings, which indicate that the stress transfer from the screw to the bone is also improved as the number of threads is increased, provide additional support for using longer bone screws with eight or more threads, when applicable. Screws with trapezoidal thread profiles, and in particular those with a more flat thread angle (Fig. 3(a)), were shown to be highly stable and were able to resist substantial pull-out loads when inserted into synthetic cancellous-bone-like hard foam and into cadaveric vertebrae [27]. Since the trapezoidal profile also demonstrated the best load sharing with cancellous bone, in terms of the STP, it seems that this profile type should be preferred in the design process.

The recent histomorphological data presented by Schuller-Götzburg et al. [20], which were taken from two patients who underwent median splitting of the mandible to treat carcinoma of the mouth, can be interpreted in view of the present computational results. The specimens containing the screws (with triangular profile) were retrieved for these histomorphological analyses at reoperation (3 months post-implantation) because of local reoccurrence of the tumors. It is evident from the images presented by Schuller-Götzburg et al. that the majority of bone resorption took place around the tip of the screws, and that no bone contacts existed in most of the threads of their distal third. Resorption directly under the screw's heads and along the upper part of the shafts was minimal. These findings strongly support the behavior of the present computational simulations, which predict that most mechanical stress is transferred to the bone bounded between the head and the first (uppermost) thread of the screws, while the bone found between the distal threads carries only negligible load and is, thereby, susceptible to resorption (Figs. 5–7).

The screw–bone computational models are based upon several assumptions, which should be taken into account. First, the 2D approach put some limitations on the interpretation of the results, as the true nature of the screw–bone contact problem is 3D, mainly due to the continuous 3D spiral geometry of the real screws (the STP comparative approach is, however, applicable to more complex 3D models). Secondly, the present models did not consider the true trabecular microarchitecture of cancellous bone, and assumed it to be a homogenous isotropic material. The local effects of the screw's engineering design parameters, including the profile shape and material properties on the microstructural stress distribution within adjacent individual trabeculae could be the topic of subsequent studies. The choice of magnitude of a standardized axial tightening load for the screws may appear arbitrary. However, according to the theory of elasticity, a direct proportionality exists between external loads and internal stresses provided that the overall geometry of the structure under investigation is not significantly changed as a result of the loading. Hence, the basic STP rating that was obtained for different screw designs and different model types should not be affected

by changing the tightening force of the screws; indeed, a sensitivity analysis in which tightening forces were altered by 25% did not provide evidence for changes in STP-derived relative rating of the screw's performances.

Finally, for further testing the applicability of the present simulations and of the STP approach to serve as standard tools for evaluating and rating the biomechanical compatibilities of various bone screw fixations, animal experiments will be necessary. Bone histological specimens taken at different stages of the process of local adaptation to the presence of the implant could, in this way, be correlated with the present STP reference values, in order to confirm the importance of elimination of stress shielding in obtaining adequate osteosynthesis.

Acknowledgements

This study was supported by the 'Ela Kodesz Institute for Medical Engineering and Physical Sciences' and by the Internal Fund of Tel Aviv University, Israel. Mr M. Shabtai and Mr Y. Gotlieb are thanked for their help in developing the computational models.

References

[1] DeCoster TA, Heetderks DB, Downey DJ, Ferries JS, Jones W. Optimizing bone screw pullout force. J Orthop Trauma 1990;4:169–74.
[2] Daftari TK, Horton WC, Hutton WC. Correlations between screw hole preparation torque of insertion and pullout strength for spinal screws. J Spinal Disord 1994;7:139–45.
[3] Asnis SE, Ernberg JJ, Bostrom MP, Wright TM, Harrington RM, Tencer A, Peterson M. Cancellous bone screw thread designs and holding power. J Orthop Trauma 1996;10:462–9.
[4] Chapman JR, Harrington RM, Lee KM, Anderson PA, Tencer AF, Kowalski D. Factors affecting the pullout strength of cancellous bone screws. J Biomech Eng 1996;118:391–8.
[5] Ferrera LA, Ryken TC. Screw pullout testing. In: An YH, Draughn RA, editors. Mechanical testing of bone and the bone-implant interface. Boca Raton: CRC Press; 1999. p. 551–65.
[6] Harnroongroj T, Techataweewan A. Determination of the role of the cancellous bone in generation of screw holding power at metaphysis. Clin Biomech 1999;14:364–6.
[7] Pilliar RM, Cameron HU, Binnington AG, Szivek J, Macnab I. Bone ingrowth and stress shielding with a porous surface coated fracture fixation plate. J Biomed Mater Res 1979;13:799–810.
[8] Tomita N, Kutsuna T. Experimental studies on the use of a cushioned plate for internal fixation. Int Orthop 1987;11:135–9.
[9] Tomita N, Kutsuna T, Tamai S, Udea Y, Ikeuchi K, Ikada Y. Mechanical effects of a cushioned plate on bone fixation. Bio-Med Mater Eng 1991;1:243–50.
[10] Van Reitbergen B, Huiskes R, Weinans H, Summer DR, Turner TM, Galante JO. The mechanism of bone remodeling and resorption around press-fitted THA stems. J Biomech 1993;26:369–82.
[11] Ang KC, Das De S, Goh JC, Low SL, Bose K. Periprosthetic bone remodeling after cementless total hip replacement. A prospective comparison of two different implant designs. J Bone Joint Surg [Br] 1997;79:675–9.
[12] Haynes RC, Pöll RG, Miles AW, Weston RB. An experimental study of the failure modes of the gamma locking nail and AO dynamic hip screw under static loading: a cadaveric study. Med Eng Phys 1997;19:446–53.
[13] American Academy of Orthopaedic Surgeons, 2000 (http://www.aaos.org:80/cgi-bin/print_hit_bold.pl/wordhtml/2000news/c9-17.htm)
[14] Lowery GL, McDonough RF. The significance of hardware failure in anterior cervical plate fixation. Patients with 2- to 7-year follow-up. Spine 1998;23:181–7.
[15] Goodacre CJ, Kan JY, Rungcharassaeng K. Clinical complications of osseointegrated implants. J Prosthet Dent 1999;81:537–52.
[16] McGlumphy EA, Mendel DA, Holloway JA. Implant screw mechanics. Dent Clin North Am 1998;42:71–89.
[17] Heller JG, Silcox 3rd. DH, Sutterlin 3rd. CE. Complications of posterior cervical plating. Spine 1995;20:2442–8.
[18] Miclau T, Holmes W, Martin RE, Krettek C, Schandelmaier P. Plate osteosynthesis of the distal femur: surgical techniques and results. J South Orthop Assoc 1998;7:161–70.
[19] McCullen GM, Garfin SR. Spine update: cervical spine internal fixation using screw and screw-plate constructs. Spine 2000;25:643–52.
[20] Schuller-Götzburg P, Krenkel Ch, Reiter TJ, Plenk Jr. H. 2D-finite element analyses and histomorphology of lag screws with and without a biconcave washer. J Biomech 1999;32:511–20.
[21] Siegele D, Soltesz U. Numerical investigations of the influence of implant shape on stress distribution in the jaw bone. Int J Oral Maxillofac Implants 1989;4:333–40.
[22] Clelland NL, Ismail YH, Zaki HS, Pipko D. Three-dimensional finite element stress analysis in and around the Screw-Vent implant. Int J Oral Maxillofac Implants 1991;6:391–8.
[23] Maurer P, Holweg S, Schubert J. Finite-element-analysis of different screw-diameters in the sagittal split osteotomy of the mandible. J Craniomaxillofac Surg 1999;27:365–72.
[24] Mow VC, Hays WC. Basic orthopaedic biomechanics. Philadelphia: Lippincott-Raven, 1997.
[25] Chen SI, Chang CH, Lin RM. The effect of the pedicle screw length within the vertebral body. In: Proceedings of the Summer Bioengineering Conference of the ASME Bioengineering Division. 2001. p. 263–4.
[26] Asnis SE, Ernberg JJ, Bostrom MPG, Wright TM. Bone screw thread design and holding power. In: Proceedings of the Annual Meeting of the American Academy of Orthopaic Surgeons. 1995.
[27] Hackenberg L, Clahsen H, Halm H. Factors influencing the anchoring stability of spinal bone screws-an experimental study. Z Orthop Ihre Grenzgeb 1998;136:451–6.